Frost action and human occupation during the Late Pleistocene in the Italian Southern Alps: micromorphological evidences from the Caverna Generosa cave

Eleonora Sessa[1*], Fabio Bona[2], Lucia Angiolini[2]

[1] Università degli Studi di Genova - Dipartimento di Scienze della Terra dell'Ambiente e della Vita (DISTAV), Corso Europa 26, 16132 Genova, Italy. *Corresponding author: Eleonora.sessa@edu.unige.it

[2] Università degli Studi di Milano – Dipartimento di Scienze della Terra "A. Desio", Via Mangiagalli 34, 20133 Milano, Italy.

Abstract

The Late Pleistocene has been characterised by frequent and intense climatic oscillation, well recorded in the Caverna Generosa cave deposits. In this work, micromorphological analyses have been performed on samples from the cave where the stratigraphy is particularly well exposed and complete, in order to obtain temporal and spatial information on climate- and human-related processes during MIS3 and 4. The older layers (more than 50 ka Before Present -BP-) record a very cold time interval, where ice did not melt during the warmer season, and with little or no vegetation outside the cave. During this cold stage, probably, humans spent a short period in the cave, using bones to light the fire and, later, cave bears dug their hibernation beds in the innermost room. Subsequently (between 50 ka BP and 40 ka BP) a relatively brief climatic amelioration should have occurred, leading to the onset of ice melting during the summer season. Between 40 ka BP and 30 ka BP, loess deposited in the cave entrance, indicating cold and arid conditions in the area. After loess deposition, recovered wet conditions have re-established with freeze and thawing processes influencing the sediments.

Key words: Late Pleistocene, Italian Pre-Alps, palaeontology, micromorphology

1. Introduction

The Last Glaciation was characterized by an intense climatic instability which deeply affected marine and terrestrial ecosystems and was a major driver of biotic dispersal (VAN ANDEL, 2002; ANDERSON *et alii*, 2013; LOWE & WALKER, 2014; TIMMERMANN & FRIEDRICH, 2016). This instability is represented by fluctuations between colder periods, i.e. stadials, and warmer periods, known as interstadials (ANDERSON *et alii,* 2013), mainly driven by the bipolar seesaw Atlantic Ocean termohaline circulation, which produced profound changes in the atmosphere and ocean circulation, in the expansion and reduction of continental ice sheets, and in the biosphere (HEINRICH, 1988; LOWE *et alii*, 2008; KJELLSTRÖM *et alii*, 2010; VAN MEERBEECK *et alii*, 2011a). These are well documented by the Greenland ice cores and sea sediments, which record the last 120 ka temperature variations (VOELKER, 2002; ANDERSON *et alii,* 2013; KINDLER *et alii,* 2014; SIMONSEN

et alii, 2019). In this context, MIS (Marine Isotope Stage) 3 and 4 are respectively considered as the interval comprised between 29 and 59 calendar (cal) ka BP (VOELKER, 2002), and the interval up to ~70 ka BP (ABBOTT *et alii,* 2012). MIS 3 records the alternation between two extreme conditions: one of severe cold climates, as those in the arctic nowadays, and the other with temperatures as warm as those in the European continent of the present day (COOPE *et alii*, 1997; VAN MEERBEECK *et alii*, 2011b). Even though, MIS 4 shows, overall, moister and cooler conditions with respect to the previous interglacial period (MIS 5e) (SORIN *et alii*, 2010), MIS 3 and 4 are often considered correspondingly as interstadial and as stadial of the Last Glaciation (roughly between 11.7 ka BP and 120 ka BP, thus between the end of MIS 2 and the end of MIS 5e), since the amplitude of their intrinsic climatic variation is reduced if compared with other stages (ANDERSON *et alii*, 2013), such as MIS 2 or MIS 5e. In fact, MIS 5 climate conditions were more variable in terms of rate of recurrence and amplitude (VIEHBERG *et alii*, 2018).

The MIS 3 and 4 stratigraphic record of the Caverna Generosa cave (North Italy), revealed by numerous excavations since its discovery in 1988, is of paramount importance for the completeness of its deposits and the quantity and quality of its fossil and archaeological content - zoological and human lithic remains - which have been the object of several palaeontological and archaeological studies (BONA, 2004; BONA *et alii*, 2007, 2009; BONA & SAVOLDI, 2016). The deposits record both human and animal occupation, extremely rare in a place at such an altitude and during a glacial period. Here, we apply a new proxy to unravel MIS 3 and 4 climate change from natural archives, that is micromorphology, i.e. "the study of soil and related materials in their undisturbed state at the microscopic level" (STOOPS, 2003). This technique has proven to be successful in recognising genetic, temporal and spatial information on climate- and human-related processes important to an understanding of past environmental conditions (MCCARTHY *et alii*, 1998; MCCARTHY & PLINT 1999; SPRAFKE *et alii*, 2014; ZÁRATE *et alii*, 2000).

Frost action, i.e. "*the direct effects of freezing and thawing on earth materials*" (POLLARD, 2018, p. 540), can express as frost heave, frost wedging, frost sorting, and frost shatter. The influence ice exerts on the deposits can depend on air temperature, soil texture, depth of frost penetration and the number of freeze and thaw cycles (POLLARD, 2018; VAN VLIET-LANOË & FOX, 2018). Consequently, also the forms in which these processes can manifest may differ (PISSART, 1970; VAN VLIET-LANOË, 2013; POLLARD, 2018). Ice wedges

63 form due to cold temperatures causing thermal contraction of deposits and their consequent cracking
64 (POLLARD, 2018; VAN VLIET-LANOË & FOX, 2018). Then, water usually fills these cracks and, when
65 temperatures drop, ice blades will develop (POLLARD, 2018).

66 Ice lensing is the most frequent pattern associated to frost action and it is related to freeze and thaw cycles,
67 responsible for lenses of segregation ice (VAN VLIET-LANOË & FOX, 2018). If the rate of freezing is slow,
68 horizontal lens of ice will tend to form; instead, if freezing is rapid water forms ice crystals in the pore spaces
69 as pore ice (POLLARD, 2018). Micromorphological microstructure, groundmass and pedofeatures portray
70 effectively and help in identifying all these frost action figures (VAN VLIET-LANOË & FOX, 2018). This
71 technique has been applied in contexts where frost action is primarily responsible for the appearance and
72 sometimes the nature of the deposits studied, such as Arctic and Antarctic regions, since 1950s, and since
73 then this technique has become more and more refined (VAN VLIET-LANOE *et alii*, 2004).

74 Even if oceans and ice sheets may provide the most important continuous record, continental sites are still
75 essential to obtain high resolution reconstruction of the terrestrial ecosystems change and, at large, global
76 paleoclimatic and paleoenvironmental reconstruction of the Last Glaciation (VOELKER, 2002).

77

78 **2. The study-area**

79

80 2.1 Geological setting

81 Caverna Generosa cave is located on the Italian side of Monte Generoso, at 1450 m a.s.l., in North-Western
82 Lombardy (Como) (45°55′58″N, 9°01′40″E) (Fig. 1). During the Late Pleistocene, the area of Monte
83 Generoso was characterized by the presence of glaciers, that never actually reached the cave itself (BINI &
84 CAPPA, 1975; BINI *et alii*, 1996). Instead, the area was surrounded by the Adda's glacier during the LGM
85 (Last Glacial Maximum, roughly 17.5 ka BP), but never directly reached by it (BINI *et alii*, 1998; BINI, 2005;
86 SERVIZIO GEOLOGICO D'ITALIA, 2013).

87 Present climatic conditions are characterized by a strong daily thermal excursion and a mean annual
88 temperature of 5 ° C. Winter is dry (approx.. 290 mm), while spring and autumn are rather wet (approx. 750
89 mm) (BLANT *et al.*, 2004).

90 The cave is excavated in the Calcare di Moltrasio Formation, widespread in the surrounding area (SERVIZIO
91 GEOLOGICO D'ITALIA, 2013). It consists of grey marly limestones, with the occurrence of dark chert nodules,
92 sometimes in large quantities (SERVIZIO GEOLOGICO D'ITALIA, 2013). In the Monte Generoso area, the
93 Radiolariti del Selcifero Lombardo (radiolarites) can be also found (SERVIZIO GEOLOGICO D'ITALIA, 2013)
94 (Fig. 2). The Caverna Generosa cave karst system began to develop due to old karst processes during the
95 Oligocene (BINI & CAPPA, 1975). The cave has a development of 200 m, but only the first 80 m from the
96 entrance have been investigated in this study. Of this first part, three main parts can be distinguished: an
97 initial tunnel called Cunicolo 13-15, a small room called Saletta and a larger room indicated as Sala
98 Terminale. The sampling for micromorphological analyses was performed only in Cunicolo 13-15 and Sala
99 Terminale (Fig. 3).

100

101 2.2 Stratigraphy and chronology

102 The sampling for micromorphological analyses was performed in Cunicolo 13-15 and Sala Terminale
103 following the stratigraphic reconstruction by BONA *et alii*, (2007, 2009) and BONA & SAVOLDI (2016), here
104 revised as follows.

105

106 *Sala Terminale***.** In the newly proposed stratigraphic reconstruction (Fig. 4), fourteen different stratigraphic
107 layers have been recognized, thus with two more layers than those previously described. These two new
108 layers were recognized at the base of the succession and are identified with number thirteen and fourteen.
109 The lithostratigraphy, in general, is rather complex as the units show frequent lateral changes (BONA *et alii*,
110 2009).

111 Level 14: residue of alteration of the cave bottom, with pebbles; clay is also present, dark brown - black in
112 colour.

Level 13: about 5 cm thick. Grey to brownish red clay matrix with silt; limestone pebbles and cobbles of maximum 10 cm in diameter, usually angular. Presence of poorly preserved deer teeth.

Level 12: thickness from 25 cm to 0 in AB6. Dark brown clay silty matrix with small aggregates of 2-3 mm, limestone cobbles of about 10 cm in diameter, mostly angular. Very rare, badly preserved cave bear and deer (*Cervus elaphus,* Linnaeus 1758) bones.

Level 11: about 16 cm thick. Greyish clay matrix with millimetric aggregates (maximum size of 3-4 mm); the dominant angular limestone cobbles are maximum 10-12 cm in diameter; towards the southwest part of the section the clay content increases, the colour turns yellowish and the cobbles of Calcare di Moltrasio Formation became smaller and less frequent. Rare presence of badly preserved bones remains. At the bottom of this level, two musterian flints have been found during the 2002 and 2004 field excavations (Bona et al. 2007). Sharp transition to level 12.

Level 10: 12-18 cm thick. Dark red, with yellowish lens, silty clay matrix; limestone cobbles larger than in other levels, around 20-30 cm in diameter. Uncommon and usually badly preserved cave bear bones. Sharp transition to level 11.

Level 9: 12-20 cm thick. Dark red clay with silt matrix. Presence of altered limestone pebbles of maximum 5-6 cm in diameter. Cave bear bones are present but poorly preserved. Gradual transition to level 10.

Level 8: between 12-20 cm thick. Brown greyish clay matrix, subangular limestone cobbles of maximum 15 cm in diameter. Presence of bone remains in a poor state of conservation. Sharp transition to level 9.

Level 7: 20 cm thick. Small lens constituted of coarse gravel. It is located exclusively in conjunction with the north wall of the Sala Terminale, in sectors AA 1 bis and AB 1 bis (not shown in the figures).

Level 6: 30 cm thick. Limestone cobbles of 6-7 cm in size, presence of lenses of organic matter, rich in bones, occasionally in anatomical connection. Sharp transition to level 8.

Level 5: 20-50 cm thick. Ochre silty matrix. Presence of altered limestone pebbles and cobbles, especially in correspondence of the rocky wall; lenses of organic matter, rich in bones whose state of preservation is variable. Sharp transition to level 6.

Level 4: from 10 to 40 cm thick. Pebbles of 5 cm in size; pale red laminated silty matrix with grey-blue clay lenses (max length 25 cm, max thickness 3 cm) probably formed by dissolution of limestone blocks. Few limestone clasts with maximum diameter of 5 cm are present. Fossil bones are common. Gradual transition to level 5.

Level 3: maximum thickness of 25 cm. The framework is composed by rare 4-5 cm altered limestone pebbles and dark fragments of Calcare di Moltrasio Formation chert. Abundant paleontological remains are present; cave bear bones are common.. This interval has been divided into four parts (a, b, c, d) based on matrix differences: a- yellowish silty clay matrix; b- orange silty clay matrix; c- yellowish silty clay matrix; d- orange silty clay matrix. The level pinches out towards the northern side of the "Sala Terminale".
Level 2: about 20 cm thick. Clayey grey-yellowish matrix with few subangular limestone pebbles of about 5 cm in diameter. Rare, but well-preserved paleontological remains.

Level 1: 10 to 60 cm thick. The matrix is a grey silty clay, with 6-7 cm sub-angular limestone cobbles, sometimes larger. The boundary to level 2 is undulated. No fossils found.

Cunicolo 13-15. Seven layers are present, as already described by BONA *et alii* (2009) (fig.5).

Levels Cun II, III, IV, V and VI are very similar, they differ mainly in the matrix colour: from light grey in the upper part, it turns dark brown in level Cun VI. According to BONA *et alii* (2009, p.257): "Differences between Cun I and lower levels probably testify a sedimentation gap that could be correlated with a sudden change in climate conditions".

Level Cun I: from 10 cm to 50 cm thick. Yellowish loessic matrix. At the bottom, or at the top of Level Cun II, well-preserved brown coloured bones of *Ursus spelaeus* (ROSENMÜLLER & HEINROTH, 1994) and *Marmota marmota* (LINNAEUS, 1758). Lower boundary of the level sharp and straight.

Level Cun 0: from less than 20 cm to 50 cm thick. Grey-yellowish silty clay matrix with subangular cobbles (max 70-80 cm). Rich in fossils (probably from a Holocene intrusive phase). Sharp lower boundary.

Radiocarbon dating. As shown in BONA *et alii* (2007), six cave bear bones (*Ursus spelaeus*) from "Sala Terminale" were subjected to ^{14}C dating (made by Geographisches Institut Universität Zürich for one of the samples, and by the Utrecht University Laboratory for the other five). The results placed the uppermost six layers in an interval of time included between roughly 38 and 48 ka BP (calibrated); the lower layers showed an age exceeding the radiocarbon dating limit (Tab. 2).

For what concerns the "Cunicolo 13-15" section (Tab. 3), six additional cave bear bones were submitted to ^{14}C dating, performed by CEDAD (Facoltà di Ingegneria, Università di Lecce). In this case, samples from layers II, III and V have been dated approximately between 34 ka BP and 40 ka BP (calibrated) (BONA *et alii*, 2009).

2.3 Palaeontology and Archaeology

Palaeontology. During the thirty years of excavations, a rich collection of Upper Pleistocene macro e micro-fossils have been collected (BONA, 2004, 2005; BONA *et alii*, 2007, 2009; BONA & SAVOLDI, 2016). The large mammal fossils collection consists mainly of *Ursus spelaeus* remains. The large amount of cave bear bones is possibly due to this animal habit to spend the hibernation time in caves, where, eventually, some specimens died and left their bodies behind. This very fortunate, from a palaeontological point of view, situation allows the reconstruction of the paleoecology of different bear populations who lived for thousands of years in the area of Monte Generoso. Others very rare large mammal remains consist mainly in small to middle-size carnivores (wolves, foxes, martens exc.) and their preys (deers, moose, ibex and chamois) (BONA 2004, 2005; BONA *et alii*, 2009).

Small fossil remains consist mainly of small mammals although some fossils of reptiles, amphibians and birds have been collected too (BONA *et alii*, 2009). Small mammals have been fundamental to assess precise paleoenvironmental and paleoclimatic reconstructions of the Caverna Generosa surroundings during part of the Last Glaciation (BONA *et alii*, 2007, 2009) and to draw attention to the westward migration, not only of large faunal elements, but also of small ones (BONA & SAVOLDI, 2016).

189 *Archaeology.* During excavation campaigns, six flakes (three of them were Levallois flakes) have been
190 recovered scattered in the sediment and affected in most cases by intense post depositional alteration. They
191 are very rare, but very important items testifying incursions of *Homo neanderthalensis* (King, 1864) groups
192 equipped with Mousterian end products and radiolarite flakes, the latter from southern locations. End-
193 products prove that lithic reduction sequences were spatially and temporally active in the territory covered by
194 human groups (BONA *et alii*, 2007).

195

196 **3. Materials and methods**

197

198 3.1 Sampling

199 Undisturbed samples were collected by excavating around the desired location and covering it with plaster
200 (MILLER *et alii*, 2010). This procedure was performed in two different parts of the cave: Sala Terminale and
201 Cunicolo 13-15. Eight samples (MG 2-12) were taken in Sala Terminale, located as shown in Figure 4.
202 Given the nature of the deposit and the evident presence of bioturbation (marmot burrows) for almost all its
203 length, it was possible to sample only a single monolith (MG CUN I) from layer I of the Cunicolo 13-15
204 section (Fig. 5).

205

206 3.2 Micromorphology

207 Micromorphology involves the study of undisturbed soils, sediments, and, eventually, associated
208 archaeological materials at microscopic scale (Goldberg & Sherwood 2006). Samples collected in the field
209 were sent to the laboratory in Piombino (Massimo Sbrana – Servizi per la geologia), where they were dried,
210 impregnated with epoxy resin and finally cut in slabs of 55x95 mm, following the BENYARKU & STOOPS
211 protocol (2005). Thin sections were then analysed using a Leitz Laborlux 12 Pol microscope, with
212 magnifications 2.5-50x, under plain polarized light (PPL), crossed polarizers (XPL) and oblique incident
213 light (OIL). The description followed STOOPS (2003) and BULLOCK (1985), as well as some personal
214 additions where it was considered convenient, as already performed for Tana di Badalucco cave (SESSA *et*

215 *alii*, 2019). NICOSIA & STOOPS (2017), STOOPS *et alii*, (2010, 2018)have been utilised as a guide to feature
216 interpretation. Additionally, we adopted the terms suggested by STOOPS (2003) to describe fabric units sizes,
217 whereas we used BULLOCK (1985) and MACPHAIL & GOLDBERG (2017) tables and charts for estimations
218 and numerical data. Frequency and abundance terms are reported following MACPHAIL & GOLDBERG
219 (2017). After the description and interpretation, a synthetic approach was used to correlate the results, the
220 microfacies type concept (MFT) (GOLDBERG & MACPHAIL, 2013).

221

222 3.3 Fluorescence microscopy

223 An Olympus IX70 Fluorescence Microscope (in DISTAV laboratories, Genova) was used to detect, mainly,
224 phosphatic remains in thin sections, taking advantage of their characteristic autofluorescence (STOOPS, 2003,
225 2017). This technique was used combined with micromorphological analysis.

226

227 3.4 Radiocarbon dating calibration

228 The ^{14}C dating published so far still lacked calibration. It was decided to remedy here (Tab. 2, Tab. 3). The
229 calibration was possible thanks to the program OxCal v. 4.3.2. (Fig. 6), a simple calibration program capable
230 of building chronological models by combining dating evidences (BRONK RAMSEY, 2017). This program
231 alone cannot, however, build models applicable to every part of the world. For this reason, calibration curves
232 suitable for mid-latitudes have been used here, in particular for those of the Northern Hemisphere (IntCal13)
233 (REIMER *et alii*, 2013).

234

235 **4. Results**

236 All samples coarse fraction is characterized by the occurrence of only one mineral type, quartz. In the same
237 way, rock fragments of only one lithology (chert) have been found throughout the cave. Bone fragments are
238 present, varying significantly in their abundance, size and degree of weathering. Typical cryogenic
239 microstructures and voids are well represented in almost all samples, differing in their nature, level of

expression and preservation. Phosphates are abundant in different forms: pedofeatures, coprolites and as one of fine fraction main components, detectable by the way it affects the b-fabric appearance, making it isotropic (extinct in XPL). In a few limited cases, bioturbation and, in a lesser extent, issues encountered during thin section preparation, prevent from fully understand deposits fabric. Sometimes, it may happen that the samples undergo slight modifications due to certain procedures performed during the thin section preparation, such as an accidental increase in the dimensions of the voids with consequent alteration of the reciprocal relationships between the different basic constituents, in particular during drying.

We were able to identify four different microfacies types (MFT) in Sala Terminale, from the superior part downwards (Table 1): Frost action weakening (FAW); Bioturbation (B); Intense frost action (IFA); Arid cold stage (ACS). Only one microfacies type was recognized in Cunicolo 13-15: AI - Aeolian input. Numbers associated to thin sections roughly correspond with the stratigraphic level they derive from. Percentages, when reported, are to be intended with respect to the total thin section area. A brief summary of the descriptions can also be found in Table 1

Sala Terminale:

Frost Action Weakening MFT FAW (MG 2, MG 3, MG 5)

It is recorded by the four uppermost stratigraphic units, not considering layer one (not sampled). The MFT is characterised by a moderately separated subangular blocky microstructure, with a platy overprint (fig. 7a), and the simultaneous presence of both subangular blocky peds (1 cm medium) and porous crumbs (2 mm medium)(fig. 11a), even if in lesser amount. Voids are overall frequent and of different types: planes (10%), vughs (2%), vesicles (5%) and chambers (2%) are present. In this microfacies, some planar voids show a characteristic appearance: they are straight planes but reduced in thickness (fig. 8d). The c/f-related distribution pattern is open porphyric and the $c/f_{5\mu m}$ ratio is 1/4. Bones are rare and fine sand in size (100 μm) on average, except for two fragments 2 cm big, they show a yellowish appearance in PPL and have first-order colours birefringence. Angular and subangular quartz grains (50 μm) are very few, while angular chert fragments are few and not well-sorted (from 125 μm to few centimetres in a small number of cases). The fine

fraction is brown – light brown, mainly composed of clay and phosphates, the birefringence is weakly developed, with more mosaic speckled traits in the upper part and porostriated beneath. Occasional carnivore or omnivore coprolites (autofluorescent in FBL; Stoops, 2017) were recognised in the whole MFT (0.3 mm) (fig. 7b-c), sometimes accompanying rare cryptocrystalline apatite nodules (also autofluorescent in blue light, 75 μm) and rare impregnative microcrystalline manganese hypocoatings (75 μm).

Bioturbation MFT B (MG 3 lower part, MG 6, MG 10, MG 11)

The entire MFT is characterized by a rather chaotic arrangement of all its components (fig. 7d). The dominant microstructure is a moderately separated subangular blocky. The porosity is common (~30%) and mostly represented in equal measure by planes, vughs and channels. The coarse/fine related distribution is double spaced porphyric and the $c/f_{5\mu m}$ ratio is 2/3, denoting an increase in the coarse fraction with respect to the previous MFT. The coarse fraction consists of sand-sized bones, abundant with typical light yellow colour in PPL and first-order yellow and white in XPL, and possibly, but more analysis are needed, occasional burnt bones (but exclusively in layer 11, MG 11) (fig. 7e), with orange-red colour in PPL and second-order reddish interference colour in XPL. The coarse fraction is also composed of few or very few subangular quartz grains (60 μm), but frequent angular and subangular chert fragments (fig. 8 c-d), poorly sorted. The fine fraction components are phosphates and clay, the former conferring the typical undifferentiated b-fabric (fig. 8d). Diverse phosphatic pedofeatures are present: rare-occasional cryptocrystalline apatite nodules (175 μm), very rare limpid cryptocrystalline apatite coatings (125 μm) (fig. 8e-f) and very rare dusty capping coatings (150 μm). The remaining pedofeatures are rare manganese dendritic nodules (75 μm in diameter), sometimes associated to bones.

Intense Frost Action MFT IFA (MG 8)

The occurrence of prismatic peds (of 1 cm in size) is easily discernible also to the naked eye (fig. 9b). The microstructure is a moderately separated prismatic with a frequent porosity, mainly represented by planes (15%). Additionally, few star-shaped vughs (10%) and few mamillated vesicles (5%) are present. The c/f

related distribution is, again, open porphyric and the c/$f_{5\mu m}$ ratio is 3/7, with a decrease in the coarse fraction amount than the previous MFT (Bioturbation). The coarse material is composed of occasional medium sand sized bones (some of them fragmented in shards, with breaks in common and continuing throughout the peds) (fig. 9c-d). The mineral fraction is composed of very few angular and subangular quartz grains (50 μm) and angular chert fragments (0.5 mm). The micromass is brown and it mainly consists of clay and phosphates, making the birefringence undifferentiated. Pedofeatures seem to be completely absent.

Arid cold stage MFT ACS (MG 12)

Prismatic peds (1 cm) have been identified as well here, even if less developed than in MFT 3, together with subangular blocky peds (2 mm). The microstructure is weakly separated prismatic. The porosity is frequent, primarily in the form of planar voids (10%), subsequently as chambers (5%), channels (5%) and vughs (2%). The c/f related distribution is open porphyric (fig. 8g) and the c/$f_{5\mu m}$ ratio is 3/7. The coarse material has abundant not autofluorescent in FBL bones (medium sand-sized on average) (fig. 7f-g), rare autofluorescent in FBL bones (fig. 8g-h), very few angular quartz grains (50 μm), but common angular, not well-sorted (from 50 μm to 3 cm) chert fragments. Bones lacking in autofluorescence when observed in FBL (Fluorescent Blue Light), show orange-red colour in plain polarised light and second-order reddish birefringence with crossed nicols (fig.8g-h). These characteristics are usually associated with heating (NICOSIA & STOOPS 2017; STOOPS 2017), but only further analysis can confirm or confute this hypothesis. The reddish micromass is clayey and rich in phosphates, with an undifferentiated b-fabric (fig. 8h). Very rare manganese dendritic nodules (125 μm) are present.

Cunicolo 13-15:

Aeolian input MFT AI (MG CUN I)

The moderately separated granular microstructure (granules, 0.5 mm) is the main characterizing aspect (fig. 10e), together with the close coarse rounded rough enaulic relative distribution. Nevertheless, also crumbs are present measuring 2 mm medium and both peds types have a moderately developed pedality (fig. 8b). It

318 is common the presence of silt-sized angular and subangular quartz grains and few well-sorted angular chert
319 fragments (2 mm). Occasional bone fragments (0.1 mm) are reported. The yellowish fine fraction is mainly
320 composed of clay and phosphates (fig.8b), the birefringence is weakly developed, with an appearance typical
321 both of an undifferentiated and of a mosaic speckled b-fabric (fig. 10d). Many cryptocrystalline typic apatite
322 nodules (0.1 mm) have been recognised (fig. 10c), while only rare fragmented dense dusty microlaminated
323 clay complete infillings (150 μm) have been observed.

324

325 **5. Discussion**

326 The lowermost sampled layers of Sala Terminale (from layer 8 to layer 12) could not be dated, exceeding
327 radiocarbon dating limit (i.e. 50 ka BP) (BONA *et alii*, 2007). Nevertheless, based on field analysis
328 (sedimentological and palaeontological observations), it was possible to attribute them to the Late
329 Pleistocene. This because no trace of erosion or absence of deposition are evident, together with the fact that
330 in the lowermost levels frost signs are present and they can be easily attributed to the Last Glaciation, rather
331 than prior to that event. As shown in the results section, pedofeatures and weathering of some materials from
332 level 12 (corresponding to MFT ACS) point to weak hydromorphic conditions (STOOPS, 2003) (fig. 7h),
333 while prismatic peds can be associated to freeze and thaw (MOL *et alii*, 1993; VAN VLIET-LANOË, 2013;
334 VAN VLIET-LANOË & FOX, 2018). These two characteristics are of major importance and dwell the
335 significant information of how ice segregated in a network of vertical to sub-vertical blades, cutting the
336 deposits in prisms of 1 - 5 cm in diameter (VAN VLIET & LANGOHR, 1981). Nowadays, these structures are
337 "*observed in areas with a mean annual air temperature below -6°C*" (VAN VLIET & LANGOHR, 1981, p.140)
338 and develop by frost cracking (VAN VLIET & LANGOHR, 1981; POLLARD, 2018). Instead, the
339 sedimentological analysis of level 12 (BONA *et alii*, 2007) shows the occurrence of silt, usually associated to
340 arid climate conditions (CREMASCHI & VAN VLIET-LANOË, 1990). It may be possible that this level bears
341 also signs of human occupation, represented by what seems to be a good amount of burnt bones, probably
342 heated at a temperature around 300 °C, given their colour and the absence of autofluorescence in FBL
343 (NICOSIA & STOOPS, 2017) (fig. 7f-g). If this is confirmed by further analysis, the total absence of charcoal
344 would suggest that these bones were used as fuel in cold climate conditions and rarity of woody plants

(SCHIEGL *et alii*, 2003), as those already reconstructed by BONA *et alii* (2009). Moreover, in this same layer a Levallois lithic artefact has already been found in previous excavations (BONA *et alii*, 2007). In any case, the micromass, mainly composed of clay, does not show evidences of reddening, nor chert fragments bear any sign of heating. This concurs in indicating that if this part of the cave is actually a deposit rich in burnt bones, these were not burnt in situ, thus it probably was a dumping zone (MILLER *et alii*, 2010). Moreover, the very fragmented cervids remains, probably attributable to a species of *Cervus* (BONA *et alii*, 2009), given the probable traces of anthropogenic, but not animal frequentation, can be associated to these human groups' activities. However, given the extreme fragmentation of the remains, it is not possible to make further taphonomic observations to confirm the origin of the accumulation.

Levels 6, 10, 11 and the lower part of level 3 (MFT B), show signs of bioturbation, quite common throughout the cave. Although in the field these traces were not evident, they were discernible in thin section. The fabric, as well as the chaotic arrangement of the coarse fraction elements, indicates a certain influence exerted by animals (KEHL *et alii*, 2018). Unfortunately, it is not possible to determine whether these traces are attributable to recent or past events and exactly which animal was involved. Considering the large amount of cave bear bones found in these layers, nevertheless, it can be suggested that this sediment movement is attributable to *Ursus spelaeus* digging beds inside the cave in order to survive hibernation. Similar ground modifications have been found all over Europe and especially in cave environments located at high altitude (FOSSE *et alii*, 2004; FOSSE & PHILIPPE, 2005). In these cases, beds are dug deep in the cave, in areas protected from outside winter conditions, and concentrated, thus permitting the finding of huge bone assemblages (FOSSE *et alii*, 2004). Anyway, the study of these floors is difficult since their building is actually a combination of excavating and use of elements naturally present in the area, such as stones and ground topography (FOSSE *et alii*, 2004). It is reasonable to suppose that a similar activity would result in a chaotic relocation of deposits, comparable to that identified in the samples.

In levels 8 and 9 (also exceeding radiocarbon dating limit), characterized by MFT IFA, different traits indicate a cool period, still characterised by frost action. This is evident for the presence of prismatic peds, star shaped vughs, mamillated (due to organic matter presence) vesicles and shattered bones (MOL *et alii*, 1993; VAN VLIET-LANOË, 2013; VAN VLIET-LANOË & FOX, 2018) (fig. 9c). Prismatic peds, as discussed

above, are indicative of frost action occurring at temperatures around -6°C (VAN VLIET-LANOË & LANGOHR, 1981). Nowadays, ice wedges, responsible for the peculiar prismatic appearance of peds, are present in areas where the mean annual temperature is below -6°C and they usually develop by thermal contraction of the frozen ground (frost cracking) (VAN VLIET-LANOË & LANGOHR, 1981). This air temperature is very different from the current, which is around 5 degrees Celsius (BLANT *et al.*, 2004). If such low temperatures were present inside the cave - which maintains a stable temperature for the whole year, equal to the mean annual temperature present outside (FORD & WILLIAMS, 2013) - then also outside the cave the climatic conditions had to be severe, with little or no vegetation, as already suggested by BONA & SAVOLDI (2016). The lack of pedofeatures and, in particular, of silt cappings can be considered indicative of the absence of an annual freeze-thaw cycle, therefore the presence of ice has been more lasting over time (VAN VLIET-LANOË & LANGOHR, 1981).

Freezing begins to exert less influence in levels 2, 3, 4 and 5, but for level 3b (lower part of the MG 3 sample) where all frost traits are erased by biological activity. These layers cover an interval comprised between 47.8 ± 2.6 ka BP (upper part level 6, UtC-10763) and 39.2 ± 1 ka BP (level 2, UtC-10761) (not calibrated) (BONA *et alii*, 2007). Manganese pedofeatures identified in the samples indicate a period of humidity, but still in cold climatic conditions (STOOPS, 2003; STOOPS *et alii*, 2018). This is supported by the identification of shattered bones and the peculiar shape and distribution of voids (planes and vesicles), as well as the occurrence of a porostriated b-fabric (MG 3)(STOOPS *et alii,* 2018). Frost shattered bone suggest in situ frost comminution with low reworking of elements (TODISCO & BHIRY, 2008) and these are easily discernible from common broken bones as the different fragments fit together and the fracture planes involve also peds (VAN VLIET-LANOË, 2010). The porostriated b-fabric is often recognised associated to ice segregation (TODISCO & BHIRY, 2008; VAN VLIET-LANOË, 2010) and is indicative of the presence of pressure exerted, in this case, by ice (KÜHN *et alii*, 2018; VAN VLIET-LANOË, 2010). Moreover, in the upper part, ice-lensing and a platy overprint are visible, also to the naked eye (fig. 11b-c). These features can be related to deep seasonal freezing, also facilitated by a certain amount of water availability (CREMASCHI & VAN VLIET-LANOË, 1990). The occurrence of wet conditions at this time was already suggested by BONA *et alii* (2009), who underlined how the zoological remains recognised in these levels were typical of moist environments. If compared to the lower layers, the difference found is the onset of a seasonal cycle of

400 freezing and thawing, therefore an increase in mean annual temperatures inside and, thus more extensively,
401 outside of the cave.

402 Level 1 (dated 38,2 ± 1,4 ka BP not calibrated, UZ 2429/ ETH 4249) was not sampled, but its éboulis nature
403 is evident (fig. 11a, the level above the level 2 label). Éboulis is an autochthonous geogenic sediment
404 deriving from within the cave system, a layer of bedrock fragments derived from roof collapse (MENTZER,
405 2018), considered an evidence of cold climate conditions (CREMASCHI & VAN VLIET-LANOË, 1990;
406 SPRAFKE *et alii*, 2014; KRAJCARZ *et alii*, 2016; KARKANAS & GOLDBERG, 2017; ROUSSEAU *et alii*, 2018;).

407 Éboulis has also been found in level Cun 0, but not in level Cun I, investigated in MG CUN I sample (MFT
408 A). The level below (level Cun II) has been dated around 33 ka BP (LTL1775A, not calibrated) (BONA *et*
409 *alii*, 2009), therefore we can suppose MG CUN I to be more recent. The micromorphological analyses
410 confirmed its loessic nature (BONA *et alii*, 2009) and, in addition, it was possible to distinguish a granular
411 microstructure (fig. 10e), frequent in frost affected deposits (PAWLUK, 1988; CREMASCHI & VAN VLIET-
412 LANOË, 1990; VAN VLIET-LANOË & FOX, 2018). Loess accumulations are indicative of periglacial
413 environmental conditions, when dryness significantly enables the transport of silt grains, even over long
414 distances (ROUSSEAU *et alii*, 2018). These sediments are considered as one of the best global proxies for
415 environmental changes on land, stating the occurrence of an arid and cold climate (ROUSSEAU *et alii*, 2018).
416 After the loess deposition, water became available again. In fact, only in wet conditions aggregates tend to
417 assume a granular shape as a consequence of repeated freeze and thawing (PAWLUK, 1988). This can happen
418 where interconnected vughs are present and in a clay loam texture, oriented parallel to the freezing front
419 (PAWLUK, 1988; VAN VLIET-LANOË & FOX, 2018). Cunicolo 13-15 is located not far from the cave entrance
420 and it shows sediments that can be related to cold and arid conditions (loess), and a microstructure that points
421 to a change towards still cold conditions, but with an increase in moistness.

422

423 **Conclusions**

424 The micromorphological analyses of the cave deposits have added very detailed information to the
425 archaeological and paleontological data already acquired (BONA *et alii*, 2007, 2009), providing a robust

reconstruction of the climate and environmental change in the western sector of the Italian Southern Alps during the Late Pleistocene (MIS 3-4). The reconstructed evolution can be summarized as follows:

- Before 50 ka BP (from level 12 to level 8 in Sala Terminale) an interval of intense cold conditions is recorded by the deposit. The ice segregation signs recognised in the samples point to severe climate conditions, typical of areas with an annual mean air temperature around -6 °C. Under these conditions, ice covered a large area and remained intact for long periods. A cover of this type implies that outside the cave the situation was enabling the development of little or no vegetation. Moreover, if our burnt bones hypothesis is confirmed, man inhabited this cave for a period of time, leaving behind traces of what could have been a hearth with bones used as fuel, as in absence of woody vegetation. Indications supporting this can be also found in the presence of deer remains within level 12, possibly linked to human activities. Animals too have occupied this cave, in the past as now. One evidence is the bioturbation recognised in thin section that, together with the large amount of cave bear bones found, suggests that these animals used to dig beds inside the cave in order to survive during the coldest periods of the year, causing the observed chaotic relocation of deposits.
- Between 50 ka BP and 40 ka BP (from level 6 to level 1 in Sala Terminale) there was a short climatic and environmental amelioration affecting both faunal assemblages and cave infillings, possibly corresponding to a Dansgaard-Oeschger event (DANSGAARD *et alii*, 1993; SPÖTL & MANGINI, 2002; BONA *et alii*, 2009; ANDERSON *et alii*, 2013). The occurrence of freeze and thaw activity, represented by ice-lensing among others, suggest the occurrence of seasonal freezing inside the cave (VAN VLIET-LANOË *et alii*, 2004). This implies a difference in the ice melting recurrence from the previous layers: before 50 ka BP deposits remained frozen for long periods, whereas in this phase thawing occurred seasonally.
- Around 30 ka BP, the outer part of the cave (Cunicolo 13-15, level CUN I and CUN II) was interested by loess deposition, then affected by cryoturbation, leading to the development of a granular fabric. Loessic sediments "*typically form in a periglacial, or tundra-steppe environment*" (MARKOVIĆ *et alii*, 2007) and they are commonly used to infer climate and environmental oscillations (CREMASCHI, 1991). Likewise, the recognition of such a characteristic fabric supports the presence of cold conditions (PAWLUK, 1988; VAN VLIET-LANOË, 2010), but not as dry as before

since this microstructure necessitates of water to develop (PAWLUK, 1988). Thus, in a short period of time, we assist to a change from dry to wet conditions inside and outside the cave.

The newly acquired data indicate that during the whole Late Pleistocene (MIS 3-4) this cave has been subjected, with different degrees of intensity, to frost action, showing that these contexts are therefore ideal for reaching the maximum degree of expression of cryogenic phenomena (CREMASCHI & VAN VLIET-LANOË, 1990). This had a certain effect, not only on the deposits inside the cave, but also on those who inhabited it, although, only for a short period: cave bears, for example, as already demonstrated by BONA *et alii* (2007, 2009), used to exploit the cave mainly for hibernation, while man was forced to find a way to survive in an inhospitable environment, exploiting what he could find from inside the cave (bones) to light up a fire.

Acknowledgements

We would like to thank Dr. C. Alexander for his contribution concerning radiometric dating and its calibration, Dr. A. Briguglio and Dr. M. Piazza for their help and allowing to access their laboratory during the COVID-19 emergency. A special thanks to Prof. Trombino for the help, assistance, encouragement and suggestions. Thanks also to D. C. for his always exact observations.

Financial support provided by UNIMI (Fondi Speciali per le Ricerche Archeologiche).

References

ABBOTT, P.M., DAVIES, S.M., STEFFENSEN, J.P., PEARCE, N.J.G., BIGLER, M., JOHNSEN, S.J., SEIERSTAD, I.K., SVENSSON, A., & WASTEGÅRD, S. (2012) - *A detailed framework of Marine Isotope Stages 4 and 5 volcanic events recorded in two Greenland ice-cores.* Quaternary Science Reviews*,* **36***,* 59-77.

ANDERSON, D.E., ANDERSON, D., GOUDIE, A., & PARKER, A. (2013) - *Global environments through the quaternary: exploring evironmental change.* Oxford University Press, USA.

BENYARKU, C.A., & STOOPS, G. (2005) - *Guidelines for preparation of rock and soil thin sections and polished sections*. Departament de Medi Ambient i Ciències del Sòl, Universitat de Lleida, Lleida.

BINI, A., & CAPPA, G. (1975) - *Appunti sull'evoluzione e distribuzione del carsismo nel territorio del monte generoso (cantone ticino) in rapporto al vicino territorio comasco.* Actes Du 5° Congrès Suisse de Spéléologie*,* 61-67.

BINI, A., FELBER, M. & POMICINO, N. - (1996) - *Maximum extension of the glaciers (MEG) in the area comprised between Lago di Como, Lago Maggiore and their respective end-moraine system.* Geologia Insubrica, **1**, 65-78.

BLANT, M., MORETTI, M., DELLA TOFFOLA, R., & PIERALLINI, R. - (2004) - *La fauna olocenica del Sud delle Alpi Svizzere: Chirotteri e mammiferi terrestri tra passato e presente (Grotta del Canalone, Monte Generoso, Ticino).* Bollettino Della Società Ticinese Di Scienze Naturali, **92**, 31–44.

BONA, F. (2004) - *Preliminary analysis on Ursus spelaeus Rosenmüller & Heinroth, 1794 populations from «Caverna Generosa»* (Lombardy - Italy). Publications Du Musée Des Confluences, 2(**1**), 87-98.

BONA, F. (2005) - *I depositi del Pleistocene Superiore della Caverna Generosa (Lo Co 2694) Analisi Paleontologica ed Interpretazioni Paleoambientali*. Università degli Studi di Milano, Geology department, PhD thesis, 266 pp.

BONA, F., LAURENTI, B., & DELFINO, M. (2009) - *Climatic fluctuations during the last glacial in the North-Western lombardian prealps: the upper Pleistocene faunal assemblages of the Caverna Generosa* (Como, Italy). Rivista Italiana Di Paleontologia e Stratigrafia, 115(**2**).

BONA, F., PERESANI, M., & TINTORI, A. (2007) - *Indices de fréquentation humaine dans les grottes à ours au Paléolithique moyen final. L'exemple de la Caverna Generosa dans les Préalpes lombardes, Italie*. Anthropologie, 111(**3**), 290–320. https://doi.org/10.1016/j.anthro.2007.05.003BONA, F., & SAVOLDI, M. (2016) - *The first record of the birch mouse Sicista in the Upper Pleistocene sediments of Caverna Generosa (Como, NW Italy), with morphometrical, morphological and ecological considerations*. Rivista Italiana Di Paleontologia e Stratigrafia, 122(**2**).

BULLOCK, P. (1985) - *Handbook for soil thin section description*. Waine Research, 156 pp.

COOPE, G.R., GIBBARD, P.L., HALL, A.R., PREECE, R.C., ROBINSON, J.E., & SUTCLIFFE, A.J. (1997) - *Climatic and environmental reconstructions based on fossil assemblages from Middle Devensian (Weichselian) deposits of the river thames at South Kensington, Central London, UK*. Quaternary Science Reviews, 16(**10**), 1163-1195.

CREMASCHI, M. (1991) - *Il Suolo. Pedologia delle scienze della terra e nella valutazione del territorio.* [eds.] G. Rodolfi, M. Cremaschi. La Nuova Italia Scientifica, Roma. - ISBN 68 1644P, 428 pp..

CREMASCHI, M., & VAN VLIET-LANOË, B. (1990) - *Traces of frost activity and ice segregation in Pleistocene loess deposits and till of northern Italy: deep seasonal freezing or permafrost?* Quaternary International, **5**, 39-48.

DANSGAARD, W., JOHNSEN, S.J., CLAUSEN, H.B., DAHL-JENSEN, D., GUNDESTRUP, N.S., HAMMER, C.U., HVIDBERG, C.S., STEFFENSEN, J.P., SVEINBJÖRNSDOTTIR, A.E., JOUZEL, J., & BOND, G. (1993) - *Evidence for general instability of past climate from a 250-kyr ice-core record*. Nature, 364(**6434**), 218-220.

FORD, D., & WILLIAMS, P. (2013) - *Karst hydrogeology and geomorphology*. John Wiley & Sons Ltd, Sussex, England, 562 pp. https://doi.org/10.1002/9781118684986.

FOSSE, P., BESSON, J.-P., LABORDE, H., THOMAS-CANTIE, F., CAZENAVE, G., DELMASURE, M.C., LEVEQUE, T., LAUDET, F., & QUILES, J. (2004) - *Denning behaviour of "modern" brown bear (Ursus arctos, L.) in caves: biological and paleontological considerations from French Pyrenean sites.* In: Cahiers Scientifiques. Hors Série:Vol. **2**, 171-182. Department du Rhone - Museum, Lyon.

522 FOSSE, P., & PHILIPPE, M. (2005) - *La faune de la grotte Chauvet: Paléobiologie et anthropozoologie*.
523 Bulletin de La Societe Prehistorique Francaise. Persée - Portail des revues scientifiques en SHS.

524 GOLDBERG, P., & MACPHAIL, R.I. (2013) - *Practical and Theoretical Geoarchaeology*. John Wiley & Sons.

525 GOLDBERG, P., & SHERWOOD, S.C. (2006) - *Deciphering human prehistory through the geoarcheological*
526 *study of cave sediments*. Evolutionary Anthropology: Issues, News, and Reviews: Issues, News, and
527 Reviews, 15(**1**), 20-36.

528 HEINRICH, H. (1988) - *Origin and consequences of cyclic ice rafting in the Northeast Atlantic Ocean during*
529 *the past 130,000 years*. Quaternary Research, 29(**2**), 142-152.

530 KARKANAS, P., & GOLDBERG, P. (2017) - *Cave settings*. Encyclopedia of Geoarchaeology; Gilbert, AS, Ed.;
531 Springer: Dordrecht, The Netherlands, 108-118.

532 KEHL, M., ÁLVAREZ-ALONSO, D., DE ANDRÉS-HERRERO, M., GONZÁLEZ, P.C., GARCÍA, E., PARDO, J.F.J.,
533 MENÉNDEZ, M., QUESADA, J.M., RETHEMEYER, J., & ROJO, J. (2018) - *Towards a revised stratigraphy*
534 *for the Middle to Upper Palaeolithic boundary at La Güelga (Narciandi, Asturias, Spain). Soil*
535 *micromorphology and new radiocarbon data.* Geoarqueología, Entre Las Ciencias de La Tierra y La
536 Historia. Boletín Geológicoy Minero, 129(**1-2**), 183-206.

537 KINDLER, P., GUILLEVIC, M., BAUMGARTNER M., SCHWANDER J., LANDAIS A., & LEUENBERGER M. (2014)
538 - *Temperature reconstruction from 10 to 120 kyr b2k from the NGRIP ice core.* Climate of the Past, **10**,
539 887-902.

540 KJELLSTRÖM, E., BRANDEFELT, J., NÄSLUND, J.O., SMITH, B., STRANDBERG, G., VOELKER, A.H.L., &
541 WOHLFARTH, B. (2010) - *Simulated climate conditions in Europe during the Marine Isotope Stage 3*
542 *stadial*. Boreas, 39(**2**), 436-456.

543 KRAJCARZ, M.T., CYREK, K., KRAJCARZ, M., MROCZEK, P., SUDOŁ, M., SZYMANEK, M., TOMEK, T., &
544 MADEYSKA, T. (2016) - *Loess in a cave: Lithostratigraphic and correlative value of loess and loess-*
545 *like layers in caves from the Kraków-Czestochowa Upland (Poland).* Quaternary International, 399, 13-
546 30.

KÜHN, P., AGUILAR, J., MIEDEMA, R., & BRONNIKOVA, M. (2018) - *Textural Pedofeatures and Related Horizons.* Interpretation of Micromorphological Features of Soils and Regoliths. 377-423. Elsevier.

LOWE, J., & WALKER, M. (2014) - *Reconstructing quaternary environmentsReconstructing Quaternary Environments*. Taylor and Francis, 1-538 pp.

LOWE, J.J., RASMUSSEN, S.O., BJÖRCK, S., HOEK, W.Z., STEFFENSEN, J.P., WALKER, M.J.C., YU, Z.C., & GROUP, I. (2008) - *Synchronisation of palaeoenvironmental events in the North Atlantic region during the Last Termination: a revised protocol recommended by the INTIMATE group*. Quaternary Science Reviews, 27(**1-2**), 6-17.

MACPHAIL, R.I., & GOLDBERG, P. (2017) - *Applied Soils and Micromorphology in Archaeology*. Cambridge University Press, 631 pp.

MARKOVIĆ, S.B., OCHES, E.A., MCCOY, W.D., FRECHEN, M., & GAUDENYI, T. (2007) - *Malacological and sedimentological evidence for "warm" glacial climate from the Irig loess sequence, Vojvodina, Serbia*. Geochemistry, Geophysics, Geosystems, 8(**9**).

MCCARTHY, P.J., MARTINI, I.P., & LECKIE, D.A. (1998) - *Use of micromorphology for palaeoenvironmental interpretation of complex alluvial palaeosols: An example from the Mill Creek Formation (Albian), southwestern Alberta, Canada.* Palaeogeography, Palaeoclimatology, Palaeoecology, 143(**1-3**), 87-110.

MCCARTHY, P.J., & PLINT, A.G. (1999) - *Floodplain palaeosols of the Cenomanian Dunvegan Formation, Alberta and British Columbia, Canada: Micromorphology, pedogenic processes and palaeoenvironmental implications.* Geological Society Special Publication, 163(**1**), 289-310.

MENTZER, S.M. (2018) - *Caves and Fissures*. The Encyclopedia of Archaeological Sciences, 1-4.

MILLER, C., CONARD, N., GOLDBERG, P., & BERNA, F. (2010) - *Dumping, sweeping and trampling: experimental micromorphological analysis of anthropogenically modified combustion features*. Faculty of Science, Medicine and Health - Papers: Part A, 25-37.

MOL, J., VANDENBERGHE, J., KASSE, K., & STEL, H. (1993) - *Periglacial microjointing and faulting in Weichselian fluvio-aeolian deposits.* Journal of Quaternary Science, 8(**1**), 15-30.

572 NICOSIA, C., & STOOPS, G. (2017) - *Archaeological Soil and Sediment Micromorphology*. John Wiley &
573 Sons, 496 pp.

574 PAWLUK, S. (1988) - *Freeze-thaw effects on granular structure reorganization for soil materials of varying*
575 *texture and moisture content*. Canadian Journal of Soil Science, 68(**3**), 485-494.

576 PISSART, A. (1970) - *Les phénomènes physiques essentiels liés au gel, les structures périglaciaires qui en*
577 *résultent et leur signification climatique*. Annales de La Société Géologique de Belgique, **93**, 7-49.

578 POLLARD, W. (2018) - *Periglacial Processes in Glacial Environments In: Past Glacial Environments:*
579 *Second Edition*:537-564. Elsevier Inc.

580 RAMSEY, C. B. (1995). *Radiocarbon calibration and analysis of stratigraphy: the OxCal program.*
581 Radiocarbon, 37(**2**), 425–430. https://doi.org/10.1017/s0033822200030903

582 REIMER, P. J., BARD, E., BAYLISS, A., BECK, J. W., BLACKWELL, P. G., RAMSEY, C. B., BUCK, C. E., CHENG,
583 H., EDWARDS, R. L., FRIEDRICH, M., GROOTES, P. M., GUILDERSON, T. P., HAFLIDASON, H., HAJDAS,
584 I., HATTÉ, C., HEATON, T. J., HOFFMANN, D. L., HOGG, A. G., HUGHEN, K. A., … VAN DER PLICHT, J.
585 (2013). *IntCal13 and Marine13 Radiocarbon Age Calibration Curves 0–50,000 Years cal BP.*
586 Radiocarbon, 55(**4**), 1869–1887. https://doi.org/10.2458/azu_js_rc.55.16947

587 ROUSSEAU, D.-D., DERBYSHIRE, E., ANTOINE, P., & HATTÉ, C. (2018) - *European Loess Records*, 1-17.

588 SCHIEGL, S., GOLDBERG, P., PFRETZSCHNER, H., & CONARD, N.J. (2003) - *Paleolithic burnt bone horizons*
589 *from the Swabian Jura: distinguishing between in situ fireplaces and dumping areas*. Geoarchaeology:
590 An International Journal, 18(**5**), 541-565.

591 SERVIZIO GEOLOGICO D'ITALIA (2013) - PROGETTO CARG. *Carta Geologica d'Italia, Scala 1: 50,000,*
592 *Sheets 075 Como*.

593 SESSA, E., RELLINI, I., TRAVERSO, A., MOLINARI, I., MONTINARI, G., ROSSI, G., & FIRPO, M. (2019) -
594 *Microstratigraphic Records as Tools for the Detection of Climatic Changes in Tana di Badalucco Cave*
595 *(Liguria, NW Italy).* Geosciences, 9(**6**), 276.

596 SIMONSEN, M.F., BACCOLO, G., BLUNIER, T., BORUNDA, A., DELMONTE, B., FREI, R., GOLDSTEIN, S.,

597 GRINSTED, A., KJÆR, H.A., SOWERS, T., SVENSSON, A., VINTHER, B., VLADIMIROVA, D., WINCKLER,
598 G., WINSTRUP, M., & VALLELONGA, P. (2019) - *East Greenland ice core dust record reveals timing of*
599 *Greenland ice sheet advance and retreat*. Nature Communications, 10(**1**), 1-8.

600 SORIN, L., ANTON, V., MIRYAM, B.M., ROI, P., & AMOS, F. (2010) - *Late Pleistocene palaeoclimatic and*
601 *palaeoenvironmental reconstruction of the Dead Sea area (Israel), based on speleothems and cave*
602 *stromatolites.* Quaternary Science Reviews, 29(**9-10**), 1201-1211.

603 SPÖTL, C., & MANGINI, A. - (2002) - *Stalagmite from the Austrian Alps reveals Dansgaard-Oeschger events*
604 *during isotope stage 3: Implications for the absolute chronology of Greenland ice cores*. Earth and
605 Planetary Science Letters.

606 SPRAFKE, T., THIEL, C., & TERHORST, B. (2014) - *From micromorphology to palaeoenvironment: The MIS*
607 *10 to MIS 5 record in paudorf (Lower Austria).* Catena, **117**, 60-72.

608 STOOPS, G. (2003) - *Guidelines for analysis and description of soil and regolith thin sections.* Soil Science
609 Society of America, 208 pp.

610 STOOPS, G. (2017) - *Fluorescence microscopy*. Archaeological Soil and Sediment Micromorphology, 393-
611 397.

612 STOOPS, G., MARCELINO, V., & MEES, F. (2010) - *Interpretation of Micromorphological Features of Soils*
613 *and Regoliths*. Elsevier, 753 pp.

614 STOOPS, G., MARCELINO, V., & MEES, F. (2018) - *Interpretation of Micromorphological Features of Soils*
615 *and Regoliths*. Elsevier, 1002 pp.

616 TIMMERMANN, A., & FRIEDRICH, T. (2016) - *Late Pleistocene climate drivers of early human migration.*
617 Nature, 538(**7623**), 92-95.

618 TODISCO, D., & BHIRY, N. (2008) - *Micromorphology of periglacial sediments from the Tayara site, Qikirtaq*
619 *Island, Nunavik (Canada).* Catena, 76(**1**), 1-21.

620 VAN ANDEL, T.H. (2002) - *The Climate and Landscape of the Middle Part of the Weichselian Glaciation in*
621 *Europe: The Stage 3 Project.* Quaternary Research, 57(**1**), 2-8.

622 VAN MEERBEECK, C.J., RENSSEN, H., ROCHE, D.M., WOHLFARTH, B., BOHNCKE, S.J.P., BOS, J.A.A.,
623 ENGELS, S., HELMENS, K.F., SÁNCHEZ-GOÑI, M.F., SVENSSON, A., & VANDENBERGHE, J. (2011a) -
624 *The nature of MIS 3 stadial-interstadial transitions in Europe: New insights from model-data*
625 *comparisons.* Quaternary Science Reviews, 30(**25-26**), 3618-3637.

626 VAN MEERBEECK, C.J., RENSSEN, H., ROCHE, D.M., WOHLFARTH, B., BOHNCKE, S.J.P., BOS, J.A.A.,
627 ENGELS, S., HELMENS, K.F., SÁNCHEZ-GOÑI, M.F., SVENSSON, A., & VANDENBERGHE, J. (2011b) -
628 *The nature of MIS 3 stadial-interstadial transitions in Europe: New insights from model-data*
629 *comparisons.* Quaternary Science Reviews, 30(**25-26**), 3618-3637.

630 VAN VLIET-LANOË, B. (2010) - *Frost Action* In: Interpretation of Micromorphological Features of Soils and
631 Regoliths:81-108. Elsevier.

632 VAN VLIET-LANOË, B. (2013) - *Cryosphère*. *Histoire et Environnements de Notre Ère Glaciaire, Ed.*
633 *Vuibert*, 444.

634 VAN VLIET-LANOË, B., & FOX, C.A. (2018) - *Frost action* In: Interpretation of micromorphological features
635 of soils and regoliths:575-603. Elsevier.

636 VAN VLIET-LANOË, B., FOX, C.A., & GUBIN, S. V (2004) - *Micromorphology of cryosols* In: Cryosols:365-
637 390. Springer.

638 VAN VLIET-LANOË, B. & LANGOHR, R. (1981) - *Correlation between fragipans and permafrost with special*
639 *reference to silty Weichselian deposits in Belgium and northern France.* Catena, 8(**2**), 137-154.

640 VIEHBERG, F.A., JUST, J., DEAN, J.R., WAGNER, B., FRANZ, S.O., KLASEN, N., KLEINEN, T., LUDWIG, P.,
641 ASRAT, A., LAMB, H.F., LENG, M.J., RETHEMEYER, J., MILODOWSKI, A.E., CLAUSSEN, M., &
642 SCHÄBITZ, F. (2018) - *Environmental change during MIS4 and MIS 3 opened corridors in the Horn of*
643 *Africa for Homo sapiens expansion*. Quaternary Science Reviews, **202**, 139-153.

644 VOELKER, A.H.L. (2002) - *Global distribution of centennial-scale records for Marine Isotope Stage (MIS) 3:*
645 *A database.* Quaternary Science Reviews, 21(**10**), 1185-1212.

646 ZÁRATE, M., KEMP, R.A., ESPINOSA, M., & FERRERO, L. (2000) - *Pedosedimentary and*

palaeoenvironmental significance of a Holocene alluvial sequence in the southern Pampas, Argentina. The Holocene, 10(**4**), 481-488.

650 ***Figure captions***

651 Figure 1 - Geographical position of Caverna Generosa cave (Como - northern Italy).

652

653 Figure 2 - Geologic sketch map of Monte Generoso and Lugano Lake showing the position of the cave. Key:
654 1 - Quaternary deposits; 2 - Eocene; 3 - Cretaceous; 4 - Upper Jurassic; 5 - Middle Jurassic; 6 - Lower
655 Jurassic; 7 - Triassic; 8 - Porfirites; 9 - crystalline basement; 10 - main faults; 11 - thrusts; 12 - urban
656 agglomerations (modified after Bona et al. 2007).

657

658 Figure 3 - Caverna Generosa cave plan.

659

660 Figure 4 - Plan and stratigraphic section of "Sala Terminale" with micromorphological samples position.

661

662 Figure 5 - Plan and stratigraphic section of "Cunicolo 13-15" with micromorphological sample position
663 (modified after Bona et al. 2009).

664

665 Figure 6 – Calibrated radiocarbon dates. The first sequence shows the Sala Terminale section dates, the
666 second Cunicolo 13-15's. Age determinations are given in calibrated years BC.

667

668 Figure 7 – Photomicrographs from the Sala Terminale sequence. (a) Photomicrograph of the evident platy
669 overprint found in sample MG2 (PPL). (b) Part of a coprolite (C) surrounded by the micromass (PPL, MG5).
670 (c) As (b) but in FBL: the coprolite is autofluorescent (MG5). (d) Photomicrograph showing the general
671 chaotic appearance found in MFT B (PPL, MG6). (e) Two little bone fragments are recognised: the one on
672 the left is reddish brown and shows the typical appearance of a burnt bone (indicated by a red arrow), the
673 other on the right, is lighter in colour (indicated by a green arrow) (PPL, MG11). (f) The microphotograph

674 shows the reddish micromass appearance of MG12 sample and a reddish bone fragment (B), recognisable
675 based on the presence of Haversian canals (PPL). (g) The same microphotograph as (f), but in FBL. Worthy
676 of note is the absence of fluorescence of the bone (B). (h) Photomicrograph of sample MG12: manganese-
677 rich pedofeatures can be found in the whole thin section and here is an example (Mn)(PPL).

678

679 Fig. 8 – Photomicrographs from the Sala Terminale sequence. (a) Photomicrograph of porous crumbs and a
680 bone fragment (left, MG2). (b) Granules and porous crumbs from MG CUN I sample. It is possible to
681 recognize its moderately developed pedality and the presence of angular and subangular quartz grains, as
682 well as the fine fraction yellowish appearance. (c) Angular and subangular chert fragments, Vughs and
683 phosphate-rich fine fraction from MG11 in PPL. (d) It is the same microphotograph as in (c), but in XPL,
684 showing the absence of birefringence. (e) Limpid cryptocrystalline apatite coating on a big chert fragment in
685 MFT B. (f) It is the same microphotograph as in (e), but in XPL, showing the absence of birefringence
686 typical for the apatite mineral. (g) Microphotograph of sample MG 12 showing the abundance of reddened
687 bones and the open porphyric c/f related distribution. (h) It is the same microphotograph as in (g), but in
688 XPL, showing the absence of birefringence and the peculiar birefringence of few bones.

689

690

691 Fig. 9 – Sample MG8 from field to microscope. (a) Field view of levels from 5 to 9 with rectangles
692 indicating the sample provenance. (b) The thin section scan shows the prismatic appearance of the sample.
693 (c) Photomicrograph of a plane void fissuring a reddish bone and continuing also through the ped (PPL). (d)
694 Photomicrograph of a brown bone fragmented in shards (PPL).

695

696 Fig. 10 – Cunicolo 13-15 and the MG CUN I sample. (a) Cunicolo 13-15 section with sampling position. (b)
697 Thin section scan of MG CUN I. (c) A little apatite nodule is indicated by a blue arrow, yellowish in PPL.
698 (d) It is the same microphotograph as in (c), but in XPL, showing the absence of birefringence, typical of
699 apatite mineral. (e) Granular microstructure and close coarse rounded rough enaulic c/f related distribution in

MG CUN I (PPL).

Fig. 11 - Sample MG3 from field to microscope. (a) Field view of the upper part of the Sala Terminale sequence. Two labels indicate the position of levels 2 and 3, above those, it is easy to identify the éboulis nature of the sediments. (b) Scan of part of the thin section. The platy appearance is distinct also at this level of magnification. (c) Microphotograph of the platy look exhibited in this sample (PPL). (d) Microphotograph of the peculiar voids aspect, correlated to cold conditions (PPL). Table 1 - Microfacies types micromorphological description synthesis. Frequency and abundance are reported following MACPHAIL & GOLDBERG (2017).

Table 2- Comparison of the multidisciplinary results from the infillings of Sala Terminale, Caverna Generosa Cave. Not calibrated dating from BONA *et alii* (2009).

Table 3 - ^{14}C dating for Cunicolo 13-15 layers. Dates are calibrated with 95,4% of reliability. Not calibrated dating from BONA *et alii* (2007).

728 Fig. 1

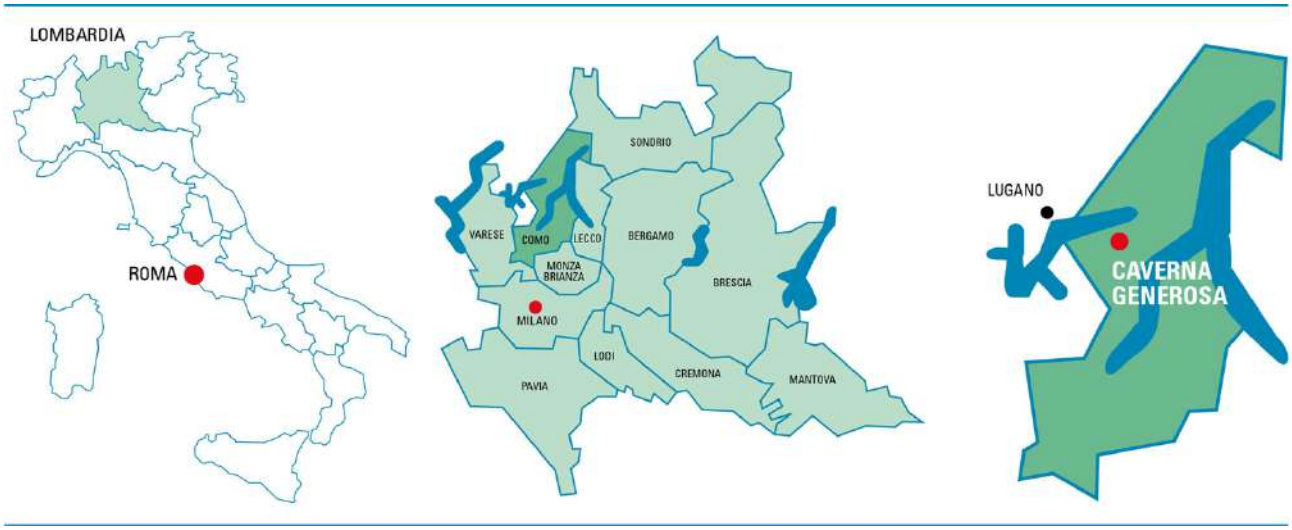

729

730

731 Fig. 2

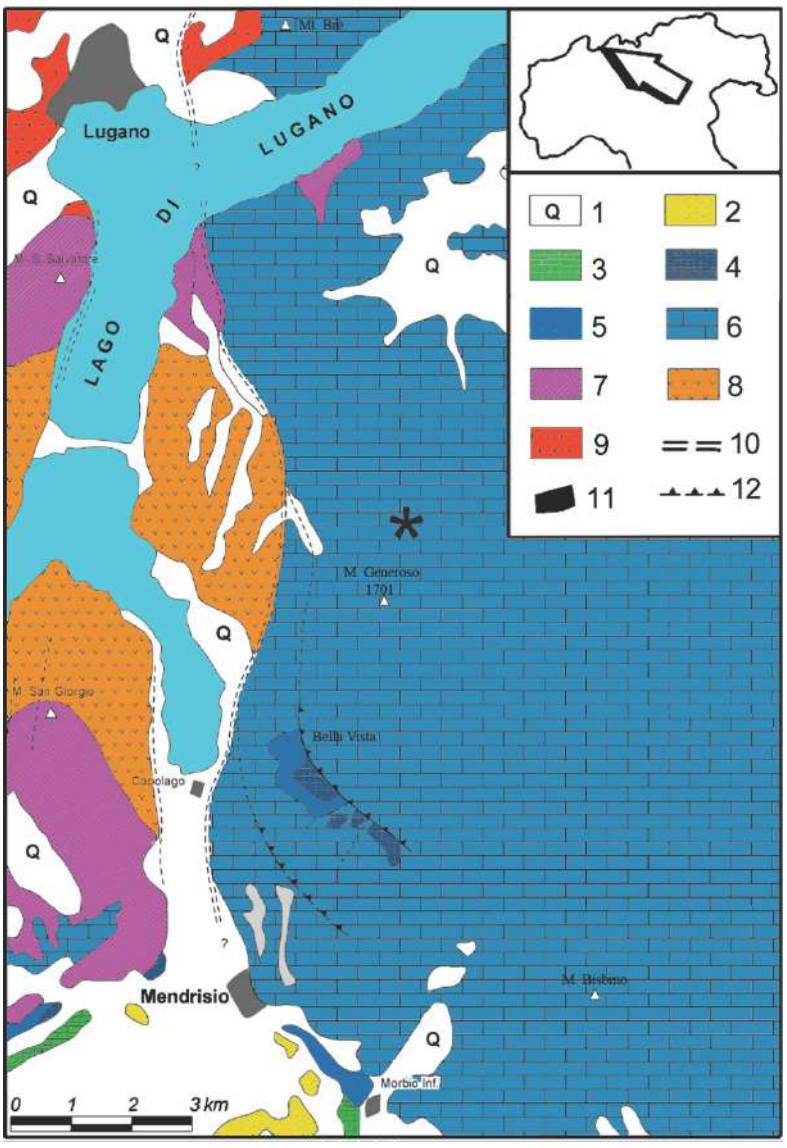

732

733 Fig. 3

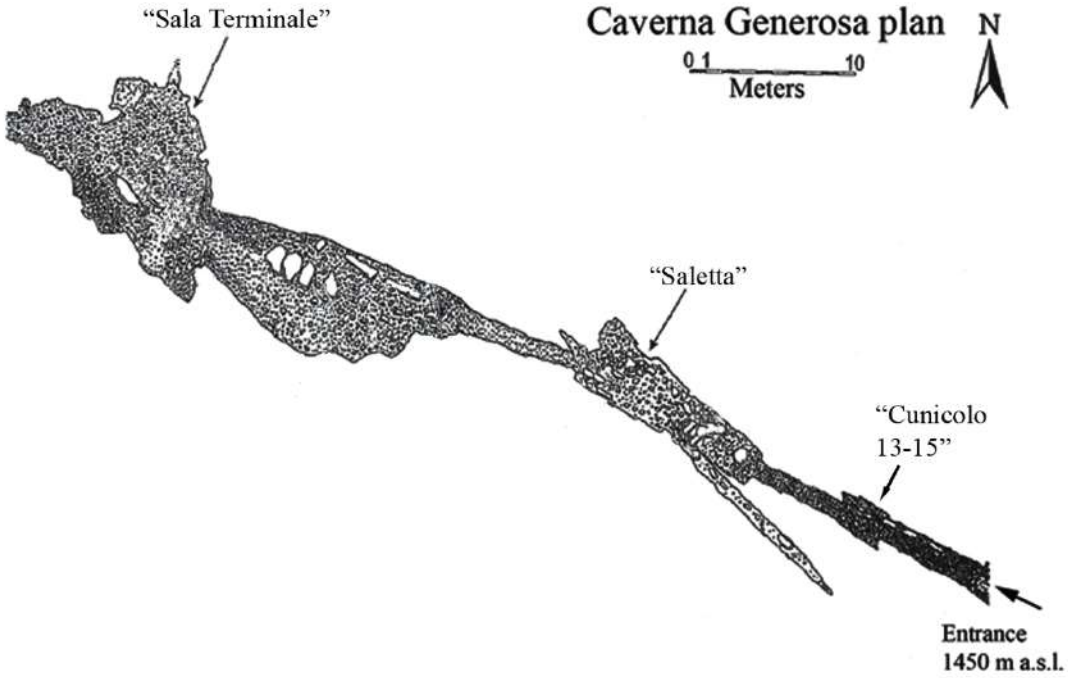

734

735

736 Fig. 4

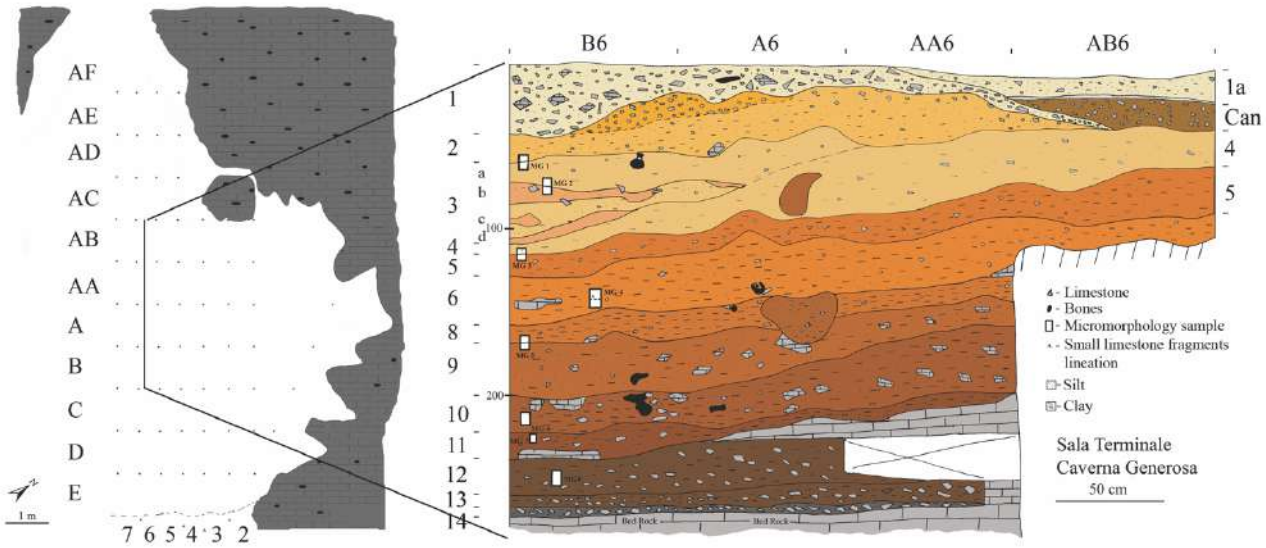

737

738

739

740

741

742

743

744 Fig. 5

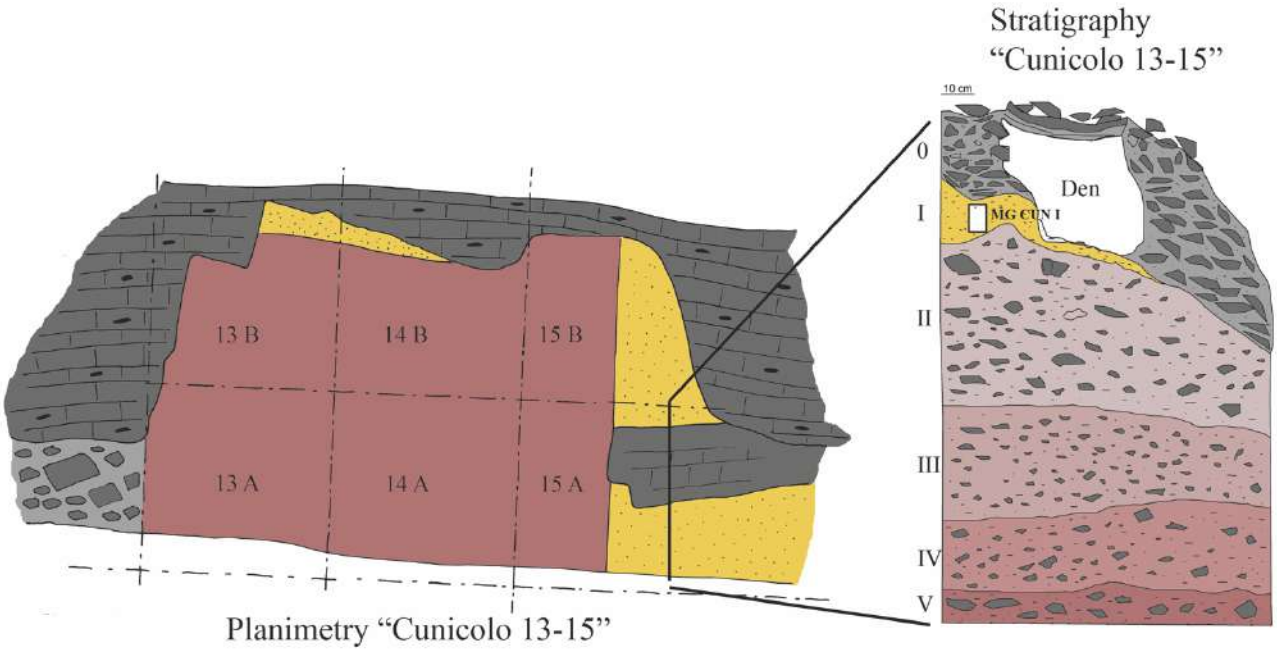

745

746

747 Fig. 6

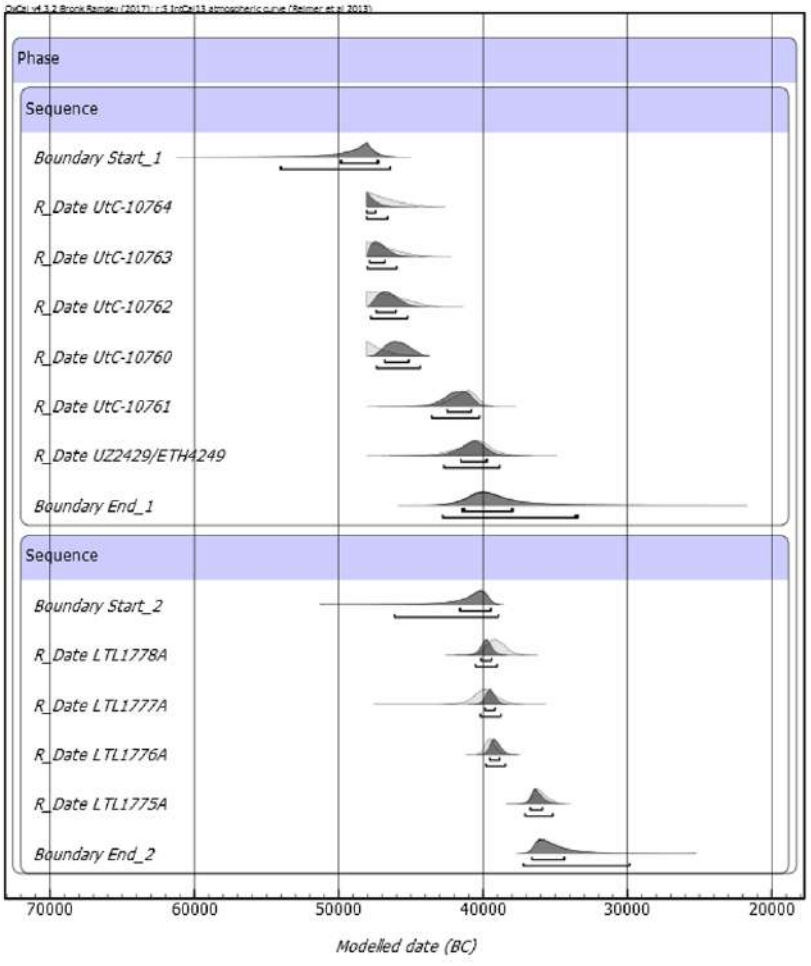

748

749 Fig. 7

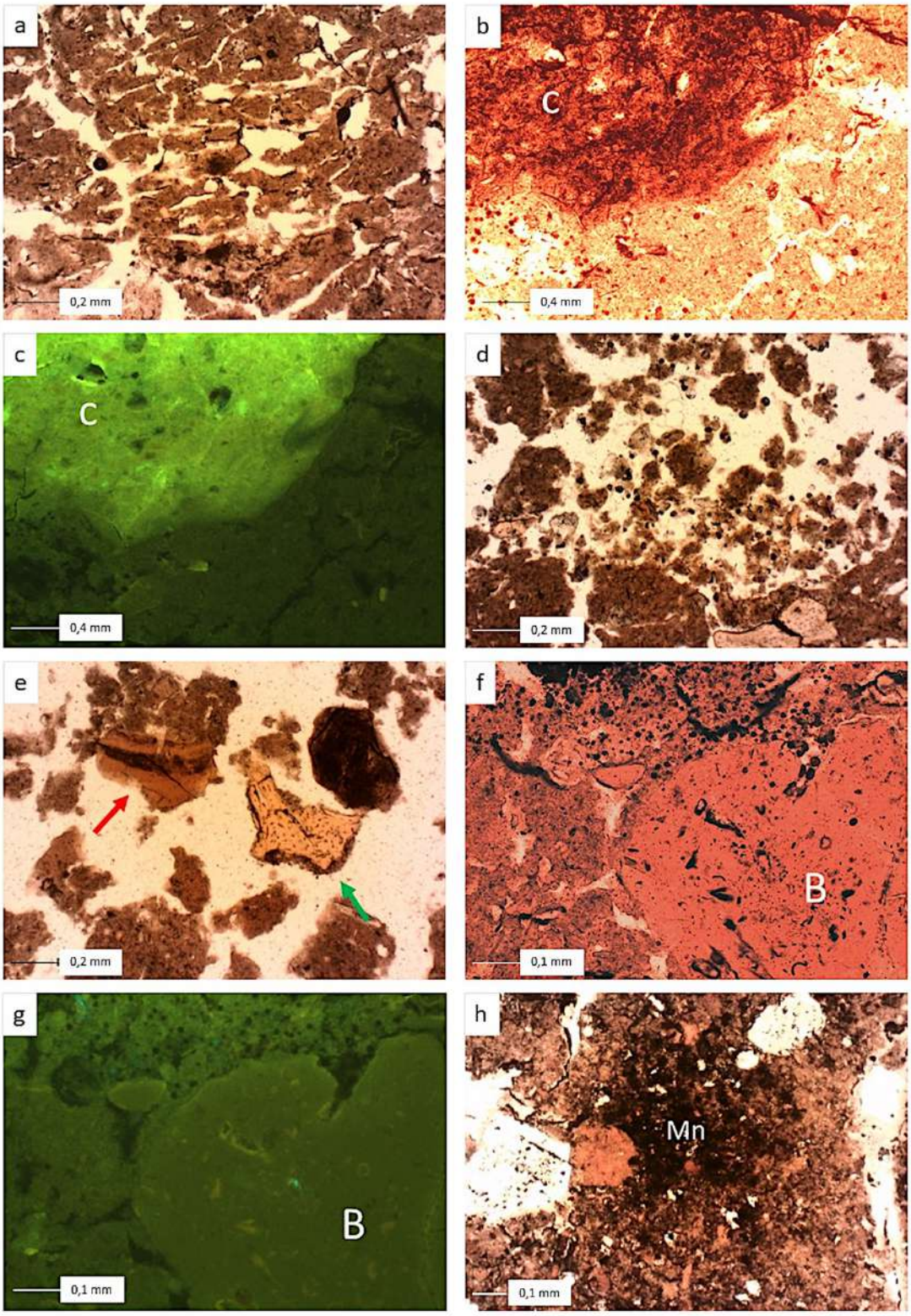

750

751

752

753

754

755 Fig. 8

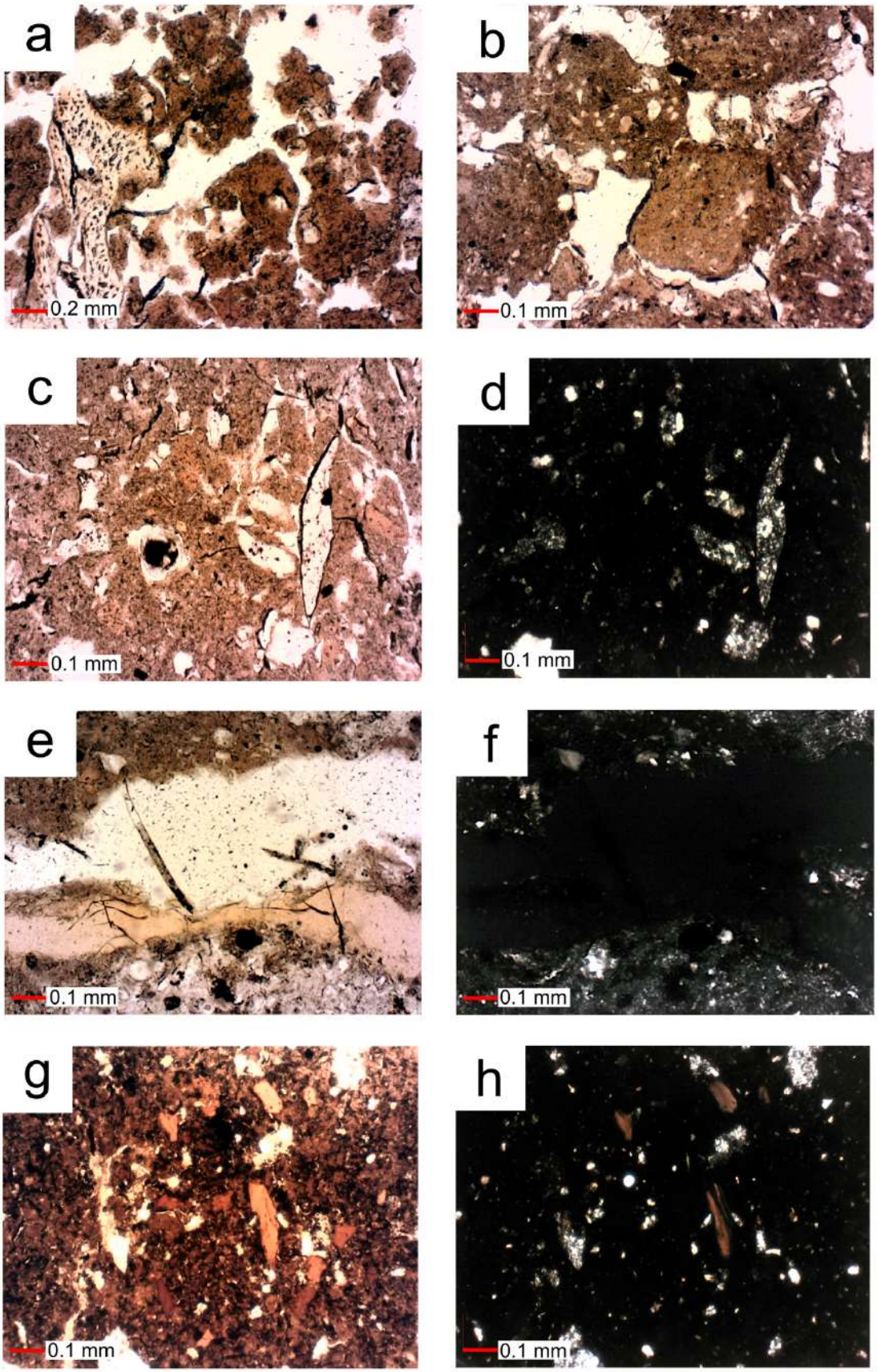

756

757 Fig. 9

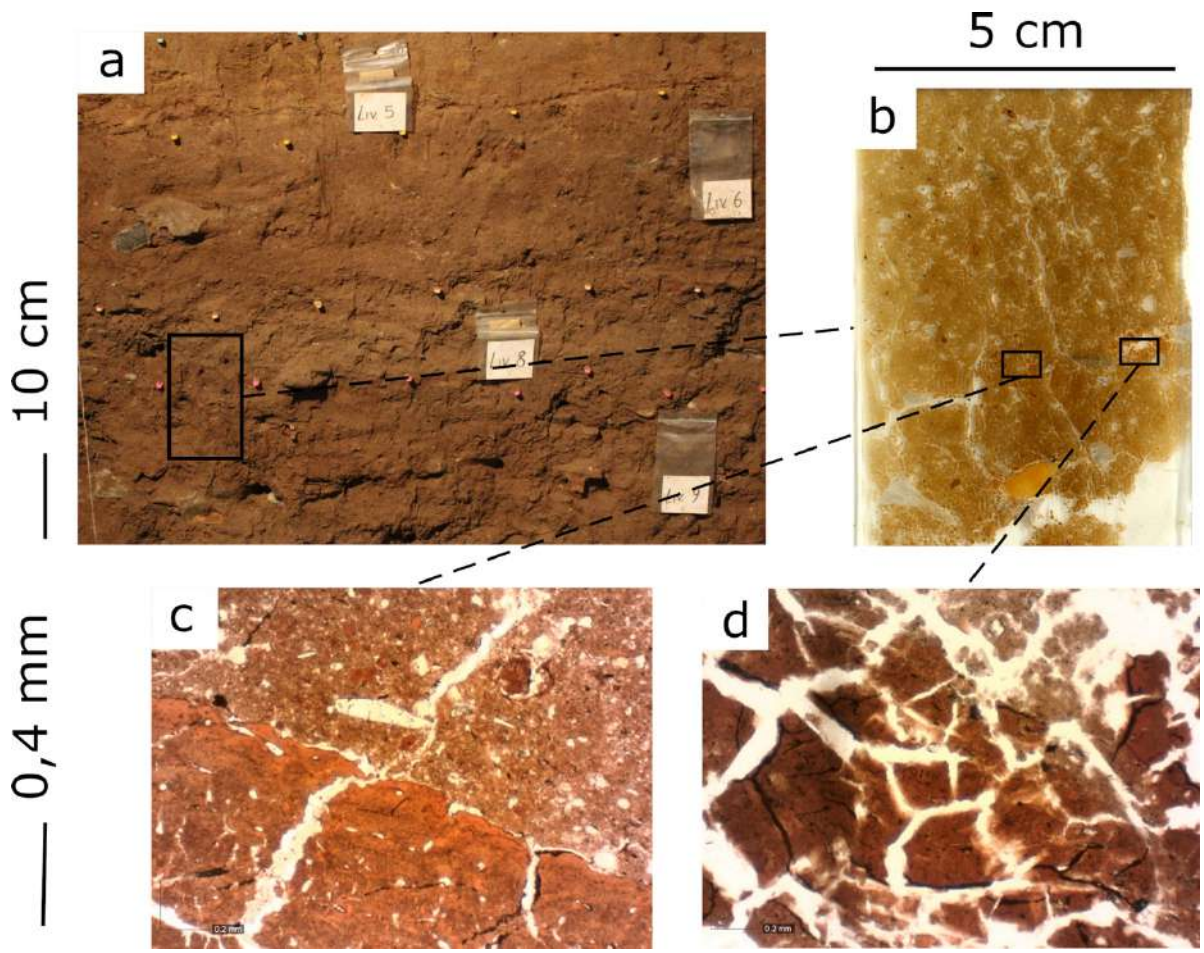

758

759 Fig. 10

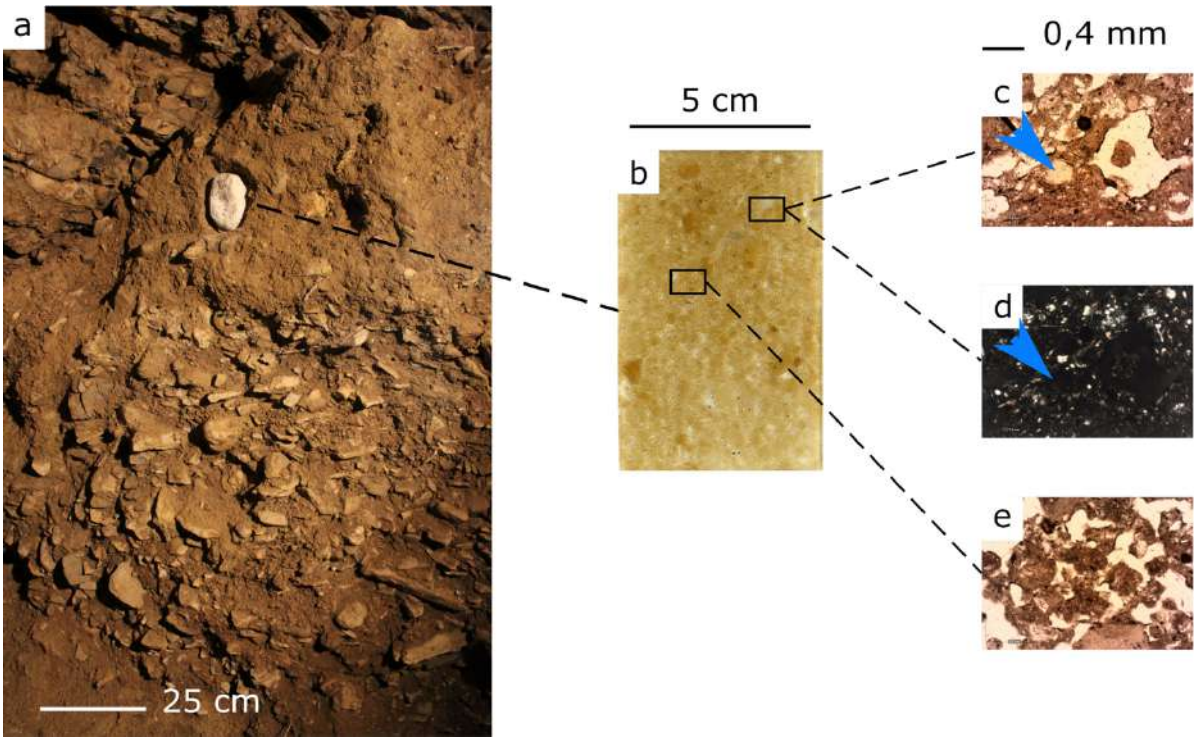

760

761

762 Fig. 11

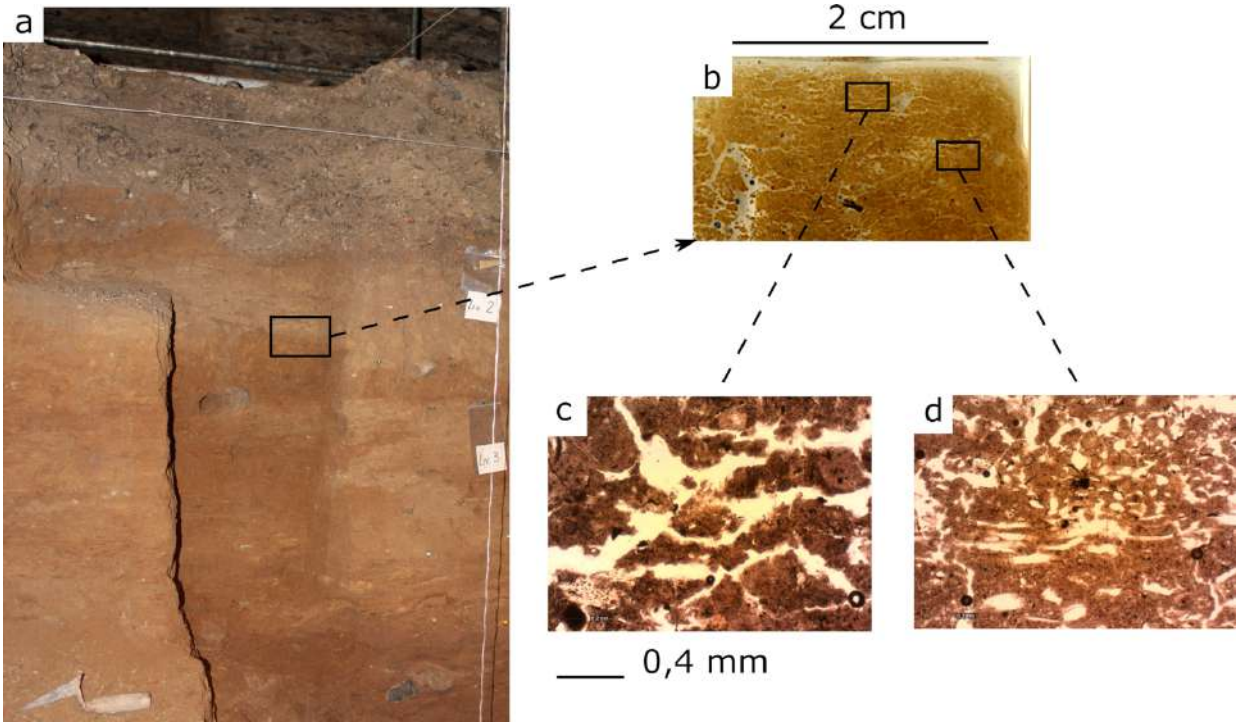

763

764

765 Tab. 1

MFT	Samples	Microstructure	Aggregates	Porosity	Dominant voids	C/f-related distribution	Coarse fraction			Fine fraction	B-fabric	Dominant pedofeatures
							Bones	Minerals (quartz)	Rock fragments (chert)			
Sala Terminale												
1 (Frost Action weakening)	MG 1, MG 2, MG 3	Moderately separated subangular blocky microstructure	Subangular blocky peds and porous crumbs	ff	Planes, vughs, vesicles, chambers	Open porphyric	a	*	f	Clay, phosphates	Weakly developed mosaic speckled (Porostriated in MG 3)	Occasional carnivore or omnivore excrements, rare cryptocrystalline apatite nodules, Mn-hypocoatings
2 (Bioturbation)	MG 4, MG 6, MG 7	Moderately separated subangular blocky microstructure	Subangular blocky peds	fff	Planes and vughs	Double spaced porphyric	aaaa	f	ff	Phosphates, clay	Undifferentiated	Rare-occasional cryptocrystalline apatite nodules, very rare limpid cryptocrystalline apatite coatings and very rare dusty capping coatings
3 (Intense Frost Action)	MG 5	Moderately separated subangular blocky microstructure	Prismatic peds	ff	Mainly planes	Open porphyric	aa	*	f	Clay, phosphates	Undifferentiated	Absent
4 (Arid cold stage)	MG 8	Moderately separated subangular blocky microstructure	weakly developed prismatic peds	ff	Mainly planes	Open porphyric	aaaaa	*	fff	Clay, phosphates	Undifferentiated	Very rare manganese dendritic nodules
Cunicolo 13-15												
A (Aeolian input)	MG CUN 1	Moderately separated granular microstructure	Granules	ff	Vesicles, channels, planes	Close coarse rounded rough enaulic	aa	fff	f	Clay, phosphates	Undifferentiated /mosaic speckled	Many cryptocrystalline typic apatite nodules, rare fragmented dense dusty microlaminated clay complete infillings

Table 1 - Microfacies types micromorphological description synthesis. Frequency and abundance are reported following Macphail & Goldberg (2017).

766

767 Tab. 2

Table 1- Comparison of the multidisciplinary results from the infillings of Sala Terminale, Caverna Generosa Cave. Not calibrated dating from Bona et al. (2009).

Level no.	^{14}C Dating (ka BP, not calibrated) (Bona et al. 2009)	^{14}C Dating (years BC, calibrated) (95,4% of reliability) to-from	Archaeological Material (Bona et al. 2007)	Faunal remains (Bona et al. 2009)	MFT (micromorphological analysis)
1	38,2 ± 1,4	38250 - 41543		Mosaic habitat with open areas alternated to wooded ones. Wet climate.	Not sampled, éboulis
2	39,2 ± 1	39876 – 42483 47985 – 46805	Lithic artefacts		
3				Wide wooded landscapes. Wetter climate.	1 - Frost action weakening and wet conditions.
4	46,7 ± 2,4	47546 – 47397			
5					
6	47,8 ± 2,6, 50,8 ± 5	47877 – 47843 47931 – 48054		Open areas with exposed rocks and reduced wooded land. Cold and dry climate.	2 - Bioturbation
8					3 - Intense frost action
9					
10				Insufficient data	2 – Bioturbation
11			Lithic artefacts		
12			Lithic artefacts	Not investigated	4 – Arid cold stage

768

769

770 Tab. 3

Table 1 - ^{14}C dating for Cunicolo 13-15 layers. Dates are calibrated with 95,4% of reliability. Not calibrated dating from Bona et al. (2009).

Sample name	Sector/level	^{14}C dating non calibrated (years BP)	To (years BC)	From (years BC)
LTL1775A	MGCUN 14A/II	33762 ± 330	34988	36717
LTL1776A	MGCUN 2 14A/II	36870 ± 400	38736	39538
LTL1777A	MGCUN 13A/II	37375 ± 1000	38070	39857
LTL1778A	MGCUN 14A//III	36479 ± 650	37891	40129

771